

ELECTRONIC TRANSPORT PROPERTIES IN a-Si:H, $\mu\text{c-Si:H}$ AND $\mu\text{c-SiGe:H}$ FILMS STUDIED BY TRAVELING WAVE METHOD

K. Chen, S. Huang, J. Xu, X. Huang, H. Fritzsche^a, A. Matsuda^b, G. Ganguly^b

National Laboratory of Solid State Microstructures and Department of Physics,
Nanjing University, Nanjing 210093, China

^aEnergy Conversion Devices, Inc., Troy, Michigan 48084, USA

^bNational Institute of Advanced Industrial Science and Technology,
Tsukuba 305-8565 JAPAN

We review our work on drift-mobility and electronic conduction measurements in a-Si:H, $\mu\text{c-Si:H}$ and $\mu\text{c-SiGe:H}$ films by traveling wave method. The change of transport mechanism in $\mu\text{c-Si:H}$ films induced by H_2 -diluted silane plasma was discussed and related to the microstructure. Also, we found that the crystallinity and grain size exerted a strong influence on the transport mechanism in $\mu\text{c-SiGe:H}$ films. Especially with very high hydrogen dilution ($R>300$), both of conductivity and mobility came to decrease, which were different from that of normal $\mu\text{c-SiGe:H}$ films. These novel phenomena were discussed by strong scattering of the potential barriers between the crystallites.

(Received July 15, 2002; accepted July 22, 2002)

Keywords: Electronic transport properties, a-Si:H, $\mu\text{c-Si:H}$, $\mu\text{c-SiGe:H}$, Traveling wave method

1. Introduction

The traveling wave method which was first introduced by Adler, Janes, Hunsiger, and Datta, enables one to determine the drift mobility of electrons and holes in certain semiconductors for which other methods are not reliable or appropriate[1-3]. For instance, the Hall effect method required the longer mean free paths than exist in amorphous semiconductors, and the time-of-flight (TOF) technique is not applicable when the materials are fairly conducting or possess very short drift ranges for excess carriers.[4,5]

Adler et al.[1] placed a thin semiconductor film a short distance above a piezoelectric crystal in the fringe electric field of a surface-acoustic Rayleigh wave. The traveling electric wave produces in the direction of its propagation a dc acoustoelectric short-circuit current or open-circuit voltage in the semiconductor film which can be measured by placing two electrodes strips separated by L across the film. The acoustoelectric voltage is proportional to the mobility of the majority carriers.

In this paper, we review our work on drift-mobility and electronic conduction in amorphous and microcrystalline ($\mu\text{c-}$) semiconductor films by traveling wave method. After we introduce the mobility measurements in n-type and p-type a-Si:H films using this method, we study the effect of hydrogen dilution on electron properties in $\mu\text{c-Si:H}$ films. Under those hydrogen dilution conditions, a change of the transport mechanism from the temperature-dependent drift mobility has been detected. The dependence of the electronic properties on the microstructure induced by the presence of hydrogen-diluted silane plasma during the deposition is discussed.

Finally, we investigate the electronic transport properties in $\mu\text{c-SiGe:H}$ films prepared by using very high hydrogen-diluted reactant gases. It was found that the electronic transport properties of our samples were quite different from that of the normal one. These novel phenomena were explained by strong scattering of the potential barriers between the crystallites.

2. Theoretical Considerations

Since the wave travels with the sound velocity V_s one can use the quasistatic approximation and obtain the field \mathbf{E} from a scalar potential: $\mathbf{E} = -\nabla\phi$. In a-Si:H the diffusion term is negligible so that $\nabla^2\phi=0$ and no space charge wave is produced. Choosing the coordinates as shown in the insert of Fig.1, The Z axis along the direction of wave propagation and the Y axis normal to the surface of the piezoelectric crystal, we write the solution of the Laplace equation in the semiconductor as

$$\phi = \phi_0 [A \cosh k(y-h) - B \sinh k(y-h)] \exp i(\omega t - kz) \quad (1)$$

With the proper boundary conditions at the air and substrate interfaces we find

$$A = [\cosh(kh) + \epsilon^* (B/A) \sinh(kh)]^{-1} \quad (2)$$

$$B/A = (\epsilon_s + \epsilon^* kd) / (\epsilon^* + \epsilon_s kd) \quad (3)$$

$$\epsilon^* = \epsilon - i4\pi\sigma/\omega \quad (4)$$

Here ϵ , σ and d are the dielectric constant, conductivity and thickness of semiconductor, h is its separation from the surface of the piezoelectric crystal and ϵ_s is the dielectric constant of the insulating substrate. The Y component of the electric field, $E_y = -\partial\phi/\partial y$, yields a current σE_y in the semiconductor film which produces two surface charge waves of opposite phase. Multiplying these with the carrier mobility μ and the Z component of the electric field, $E_z = -\partial\phi/\partial z$, one obtains two opposing surface currents [3] whose time averages are finite:

$$I_1 = \sigma(\mu/V_s) w k^2 (A \bullet B) \phi_0^2 / 2 \quad (5)$$

$$I_2 = -I_1 + \sigma(\mu/V_s) d w k^2 (|A|^2 + |B|^2) \phi_0^2 / 2 \quad (6)$$

where V_s is the wave velocity, w and d are the width and thickness of the film. The potential ϕ_0 at the surface of the piezoelectric crystal is given by the Rayleigh wave power.[6] Subscripts 1 and 2 refer to the film surface close and facing away from the piezoelectric crystal, respectively. The complex coefficients A and B are determined by the boundary conditions. Fig.1 shows the attenuation factors $A \bullet B$ and $(|A|^2 + |B|^2)$ as a function of $\sigma/\epsilon_0\epsilon\omega$, the ratio of the dielectric relaxation frequency in the film and ω . The curves were calculated for a distance $h=11\mu\text{m}$, a thickness $d=1\mu\text{m}$ and a dielectric constant of the glass substrate of 5.75. Dividing the net current I_1+I_2 by the film conductance we obtain the dc open-circuit acoustoelectric voltage:

$$V_{ae} = \pm(\mu/v_s) L k^2 (|A|^2 + |B|^2) \phi_0^2 / 2 \quad (7)$$

We now turn to the interpretation of the mobility μ . Only a fraction of δ_f/δ of the carriers in the charge wave moves in transport states which are characterized by a microscopic mobility μ_0 . Hence the mobility in Eqs. (5)-(7) is a drift mobility $\mu = \mu_0 \delta_f/\delta$. The remaining fraction $1 - \delta_f/\delta = \delta_t/\delta$ may be trapped in surface states and in localized bulk states. In the following we shall neglect surface states and discuss the traveling-wave drift mobility for amorphous semiconductors in terms of the theory of dispersive transport [7,8] and compare our results with those of TOF experiments[4]. We assume an exponential tail of localized states $g(E) = g_0 \exp(E/KT)$ with a thermal emission rate $\nu_0 \exp(E/KT)$, where E is the energy below the mobility edge $E_C = 0$. Then $E_d = -KT \ln \nu_0/\nu$ is the demarkation energy above which electrons can equilibrate with E_C at the measuring frequency ν . We distinguish two cases: (I) When $E_F < E_d$, $\delta_f/\delta = n_f / (n_f + n_t)$; n_f and n_t are the equilibrium densities of free and trapped electrons above E_d respectively. (II) When $E_F > E_d$ the traveling charge wave modulates the position of E_F and $\delta_f/\delta = [dn_f/dE_F] / [dn/dE_F]$.

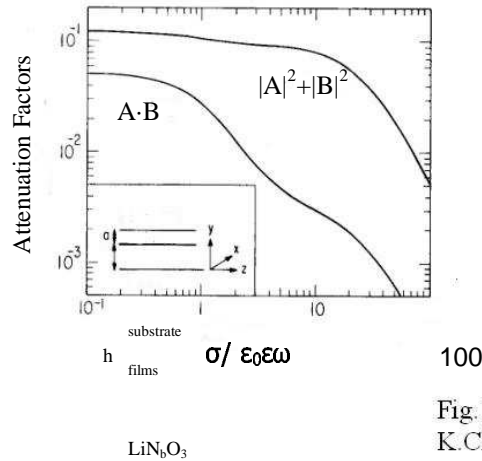

 Fig. 1
 K.Chen

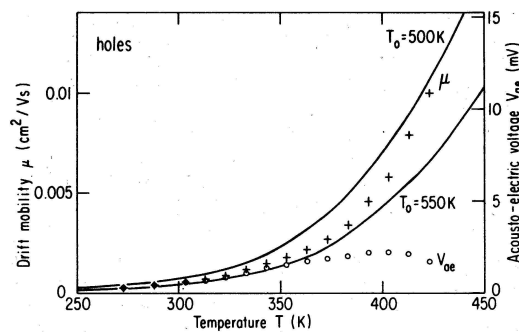
 Fig. 1. Attenuation factors as a function of $\sigma/\epsilon_0\epsilon\omega$.

Our experimental setup is identical to that of Adler et al.[1] We used a y-z cut LiNbO_3 crystal plate. The Rayleigh wave of frequency $\nu=18.2$ MHz was 0.7 cm wide. The wave velocity in the z direction is $V_S=3.488 \times 10^5$ cm/s. $1\mu\text{m}$ thick a-Si:H films were deposited on Corning 7059 substrates at $T_s=540$ K in our capacity coupled glow discharge reactor. The films having a width $w=0.7$ cm and length $L=1$ cm were separated from the LiNbO_3 surface by $h=11\mu\text{m}$ thick Capton spacers. Measurements were carried out in a flow of dry nitrogen after annealing the films at 475 K for 1 h in darkness. We found that V_{ae} is proportional to the Rayleigh wave power $P_R=0.22$ W. This corresponds in our geometry to a field amplitude $E_z=k|A|\phi_0=760$ V/cm when $\sigma < \epsilon \omega/4\pi$. At large σ the factor $|A|$ decreases according to Eqs.(2)-(4).

3. Results and Discussion

3.1. Drift-mobility and conductivity in a-Si:H films

Figs. 2 and 3 show the dc voltage V_{ae} and the corresponding drift mobilities μ obtained from Eq. (7) for holes and electrons, respectively. The μ and V_{ae} values deviate at higher T because $|A|^2$ and $|B|^2$ depend on σ . The p-type film was prepared with a gas ratio $[\text{B}_2\text{H}_6]/[\text{SiH}_4]=1.5 \times 10^{-4}$ and had $E_a=0.37$ eV. The n-type film was prepared with $[\text{PH}_3]/[\text{SiH}_4]=3 \times 10^{-4}$ and had $E_a=0.19$ eV. The solid curves drawn through the mobility data points represent the prediction of the theory described above for several T_0 values for the n-type and the p-type sample, respectively.


 Fig. 2. Acoustoelectric voltage V_{ae} and drift mobility μ of p-type a-Si:H film as a function of temperature. The full lines are calculated hole mobilities for two choices of T_0 .

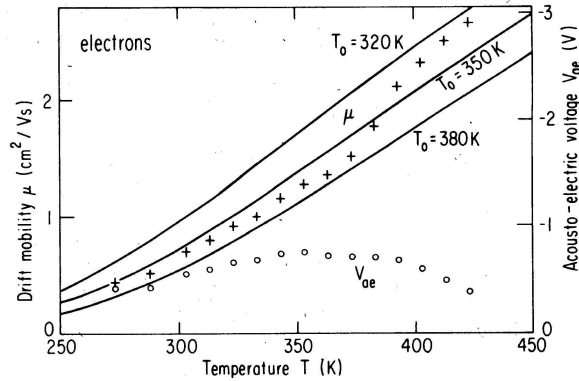


Fig. 3. Acoustoelectric voltage V_{ae} and drift mobility μ of n-type a-Si:H film as a function of temperature. The full lines are calculated hole mobilities for two choices of T_0 .

Table 1 lists our fitting parameters next to those obtained by TOF measurements [4]. The agreement is as good as can be expected since samples from different laboratories are being compared. Moreover, the currents giving rise to V_{ae} are close to the surface and interface regions of the semiconductor which may differ in structure from the bulk region which is probed by TOF measurements. In addition, the possible effect of surface states has been neglected. We also note that the TOF samples were nearly intrinsic whereas we studied doped material. Our relatively conductive samples cannot be measured by the TOF method which requires that the dielectric relaxation time is long compared with the transit time.

Table 1. Transport parameters measured by the traveling wave method and (in parentheses) by the time-of-flight technique (Ref.4).

	μ_0 (cm ² /V s)	T_0 (K)	ν_0 (10 ¹² /s)
Electrons	10±1 (13)	350±20 (312)	(0.46)
Holes	0.25±0.05 (0.67)	530±20 (500)	3 (1.6)

3.2. Change of transport mechanism in μ c-Si:H films with hydrogen dilution

The transport properties of μ c-Si:H films were also investigated by traveling wave method. The μ c-Si:H films were prepared hydrogen-diluted silane (SiH_4) plasma with the hydrogen dilution ratio $R=[\text{H}_2]/[\text{SiH}_4]$ varied from 50-500. Figure 4 shows the dark-conductivity and the drift mobility as a function of the hydrogen dilution ratio at room temperature. The σ_d has a maximum at $R=300$, which means that σ_d first increases from $(1.5\pm 0.2)\times 10^{-2}$ to $(2.9\pm 0.2)\times 10^{-2}$ S/cm then decreases to $(5.9\pm 0.2)\times 10^{-3}$ S/cm. However, μ_d monotonically increases from $(8.9\pm 0.5)\times 10^{-3}$ to $(5.5\pm 0.5)\times 10^{-1}$ cm²/Vs with increasing R .

As far as the temperature dependence of conductivity, a thermally activated conductivity was observed in all the samples. From dependence of the dark-conductivity on the temperature, we calculated activation energies, E_σ , between (104 ± 3) meV and (176 ± 3) meV. This lower activation energy is due to the fact that E_F was pinned near the conduction band by defect states in the distorted network at the transition between crystallites and the surrounding amorphous matrix according to the three-phase model [9].

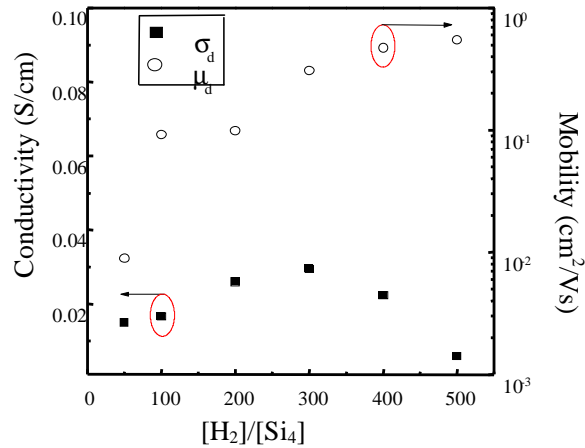


Fig. 4. The dependencies of dark-conductivity and drift mobility on hydrogen dilution ratios.

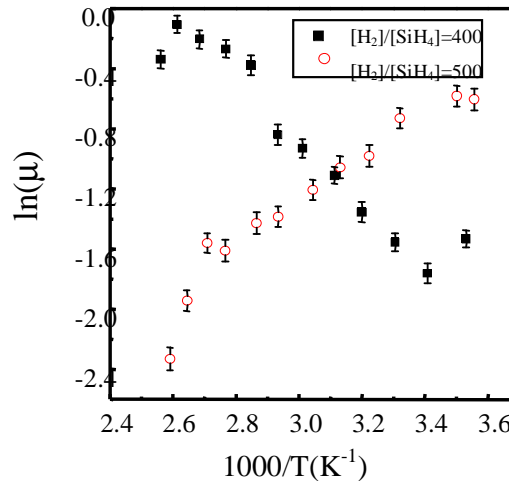


Fig. 5. The temperature dependencies of drift mobility for two samples prepared by different hydrogen dilution ratios.

For the temperature dependence of μ_d , we also observed a thermal activated process, when R varied from 50 to 400, which is similar to that in normal $\mu\text{c-Si:H}$ [10]. For R=500, however, we found μ_d decreasing with increasing the temperature, which resembled that of single-crystal silicon. The difference of temperature dependence of drift mobility is shown in Fig 5. We note that for the R of 400, μ_d increases from $(0.22 \pm 0.05) \text{ cm}^2/\text{Vs}$ to $(0.71 \pm 0.05) \text{ cm}^2/\text{Vs}$, for R=500, μ_d decreases from $(0.64 \pm 0.05) \text{ cm}^2/\text{Vs}$ to $(0.097 \pm 0.05) \text{ cm}^2/\text{Vs}$, in the region between 300 K and 400 K. From this change, we discovered that the transport properties in $\mu\text{c-Si:H}$ changed when R varied from 400 to 500.

From the temperature dependence of drift mobility, we also calculated the activation energy, E_μ , which lies between $(82 \pm 5) \text{ meV}$ and $(134 \pm 5) \text{ meV}$. Figure 6 shows the E_σ and E_μ as a function of hydrogen dilution ratio. While the R varied from 50 to 300, E_σ decreased from $(134 \pm 3) \text{ meV}$ to $(104 \pm 3) \text{ meV}$ and E_μ also decreased from $(125 \pm 5) \text{ meV}$ to $(98 \pm 5) \text{ meV}$, showing the same tendency and values as E_σ . However, with increasing R beyond 300, E_σ increased from $(104 \pm 3) \text{ meV}$ to $(176 \pm 3) \text{ meV}$, while E_μ continued to slightly decrease from $(98 \pm 5) \text{ meV}$ to $(82 \pm 5) \text{ meV}$.

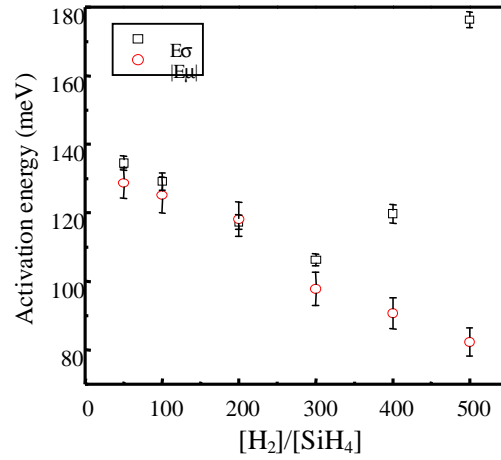


Fig. 6. The activation energy E_{σ} , E_{μ} of the samples with different hydrogen dilution ratios.

Lecomber and Grebner [9,11] concluded that the grain-boundary potential barrier has a strong influence on the transport properties in $\mu\text{c-Si:H}$ thin films. Combining this result with the XRD and Raman studies, it was revealed that there is a low amorphous phase volume and high crystalline volume fraction in the samples of our experiments. We attempt to use the evolution of the microstructures in the samples induced by hydrogen dilution to interpret the transport mechanism of our samples.

While R varied from 50 to 400, the volume fraction of amorphous phase decreased due to hydrogen plasma etching [12], consequently the distance between grains became less [13], reducing grain-boundary potential barriers. But the barriers are still not sufficiently low to allow carrier tunneling. The carriers are activated across the grain boundary as in thermionic emission. Thus the temperature dependence of μ_d is that of a thermal activated process similar to normal $\mu\text{c-Si:H}$ thin films. With increasing R to 500, the barrier becomes smaller due to a shorter distance between grains. When this distance is less than a critical distance, the carriers can tunnel directly through the barrier, which means that the carriers mainly move through crystallites. So in this range of R , we observed a decrease in μ_d with increasing the temperature as in the process of lattice scattering in the crystal. Thus, when R is smaller than 400, the transport properties are dominated by the grain-boundary potential barrier, however, when R is larger than 500, as in our experiments, lattice scattering will determine the transport mechanism.

3.3. New phenomena of electronic transport properties in $\mu\text{c-SiGe:H}$ films

Recently, the growth processes and microstructures of hydrogenated microcrystalline silicon-germanium alloys ($\mu\text{c-SiGe:H}$) have been widely investigated since these materials can be utilized in thin film transistors (TFTs), thin film solar cells as bottom cell active layer materials and other thin-film optoelectronic devices. Here, we extended our work to investigate the electronic transport properties of $\mu\text{c-SiGe:H}$ films as a function of the substrate temperature (T_s) and the hydrogen diluted ratio R defined as the ratio of hydrogen gas flow rate to the total gas flow rate of silane (SiH_4) and germane (GeH_4) ($R = [\text{H}_2]/([\text{SiH}_4] + [\text{GeH}_4])$) [14,15].

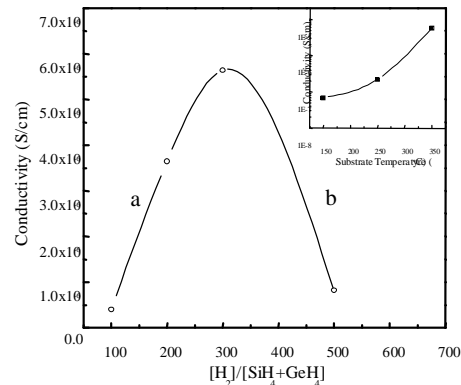


Fig. 7. The dependencies of dark-conductivity on the hydrogen diluted ratios and the substrate temperature. Solid square symbol shows the variation with R and open circle symbol shows the variation with T_s . The lines are drawn as guides for the eye.

Fig. 7 shows the room temperature dark-conductivity of μ c-SiGe:H thin films as a function of T_s and R . From the insert of Fig. 7, it can be found that the substrate temperature has a great influence on dark-conductivity by three orders of magnitude, which monotonically increases from 6.8×10^{-8} S/cm at $T_s=150$ °C to 5.64×10^{-6} S/cm at $T_s=350$ °C. However, with increasing R , the dark-conductivity only has slight change and do not change monotonically, which first increases from 4.07×10^{-7} S/cm at $R=100$ to 5.64×10^{-6} S/cm at $R=300$ and then decreases to 8.21×10^{-7} S/cm at $R=500$. When increased T_s , not only crystallinity but also grain size tends to increase continually, which lead to the pronounced increasing of conductivity in μ c-SiGe:H thin films. When the R increases from 100 to 300, the crystallinity increases but the grain size slightly decreases. In this range of R , the crystallinity increasing could be a main factor influencing on the carrier transport, which could lead to the initial increasing in conductivity as shown the region *a* in Fig. 7. However, when R increased up to 500, both the crystallinity and grain size rapidly decrease. In this case, the decrease of crystallinity and grain size runs a strong influence on the carrier transport, which could lead to conductivity decrease as shown region *b* in Fig. 7.

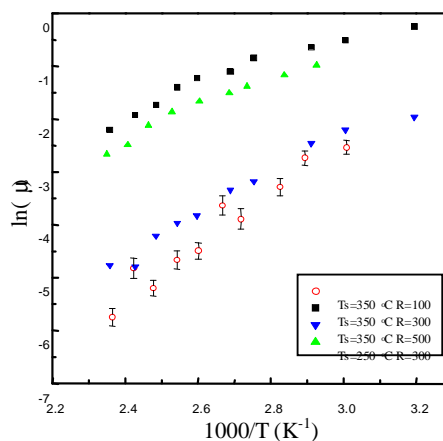


Fig. 8. The dependencies of drift mobility for three typical samples prepared by different hydrogen diluted ratios and substrate temperature, in which the values of the mobility decrease with increasing the temperature.

In the measurements of temperature-dependence of conductivity, the feature of thermal activated process was observed for all the samples. The activation energy (E_σ) values were extracted from the plot of the temperature dependence of conductivity and the value is between 0.44 eV and 0.54

eV controlling continually by changing deposition parameters. These results will be reported elsewhere.

From the sign of I_{ae} or V_{ae} , $\mu\text{-SiGe:H}$ samples are found to be weak n-type at the range of measurement temperatures. Fig. 8 shows the properties of temperature-dependence of mobility (μ_d) for different $\mu\text{-SiGe:H}$ thin films. It has been found that mobility in all the samples decreases with increasing the temperature, which is similar to the phenomena of the lattice scattering in single-crystal silicon-germanium alloy. It can be seen from Fig. 8, that slight increase in mobility can be found when T_s increased from 250 °C to 350 °C, in which R was kept constant of 300. Meanwhile changing the R from 100 to 300 great improves the drift mobility by about one order of magnitude, in which T_s is 350 °C. Then when R up to 500, the drift mobility comes to degrade.

Table 2. The changes of crystallite grain sizes (D) and germanium contents (Ge %) with substrate temperature (T_s) and hydrogen diluted ratios (R). The data of D is from the FWHM of <220> orientation in XRD spectra.

T_s (°C)	R	D (nm)	I_d
150	300	18.6	3
250		21.6	3
350		25.6	4.6
350	100	29.2	3.4
	200	24.1	4.6
	300	25.6	5.7
	500	16.4	4.7

From the results mentioned above, it can be found that substrate temperature has slight influence on the drift mobility under the same hydrogen diluted ratio, in which it seems that mobility came to be saturated. However the hydrogen diluted ratio can markedly influence the mobility under same substrate temperature. Changing the R from 100 to 300 great improving the drift mobility may be attributed to the crystallinity increasing induced by hydrogen plasma etching. Then when R grows up to 500, the drift mobility decreases, which may be ascribed to the scattering on the potential barrier between crystallites induced by the decrease of crystallinity and grain size summarized in Table 2.

4. Summary

In a summary, traveling wave method is a suitable way to investigate the transport properties of semiconductor films, especially for the materials with high resistance and low mobility. The study of the temperature-dependence of conductivity and drift mobility is helpful for understanding the electronic transport mechanism of the films based on the film composition and microstructures. This method can be extended from amorphous semiconductors to microcrystalline semiconductor materials and even to the magnetic films such as lanthanum-based transition-metal oxide perovskites [16].

References

- [1] R. Adler, D. Janes, B. J. Hunsinger, S. Datta, *Appl. Phys. Lett.* **38**, 102 (1981).
- [2] K. J. Chen, H. Fritzsche, *J. Non-Cryst. Solids* **59/60**, 441 (1983).
- [3] H. Fritzsche, K. J. Chen, *Phys. Rev.* **B28**, 4900 (1983).
- [4] T. Tiedje, J. M. Cebulka, D. L. Morel, B. Abekes, *Phys. Rev. Lett.* **46**, 1425 (1981).
- [5] M. Silver, N. C. Giles, E. Snow, M. P. Shaw, V. Cannella, D. Adler, *Appl. Phys. Lett.* **41**, 935 (1982).
- [6] B. A. Auld, *Acoustic Fields and Waves in Solids* **Vol. 2**, John Wiley and Sons, New York (1973).
- [7] J. Orenstein, M. Kastner, *Phys. Rev. Lett.* **46**, 1421 (1981).
- [8] T. Tiedje, A. Rose, *Solid State Commun.* **37**, 49 (1981).
- [9] S. Grebner, F. Wang, R. Schwarz, *Mater. Res. Soc. Symp. Proc.* **283**, 513 (1993).
- [10] D. Ruff, H. Mell, L. Tóth, I. Sieber, W. Fuhs, *J. Non-Cryst. Solids* **227-230**, 1011 (1998).
- [11] P. G. Lecomber, G. Willeke, W. E. Spear, *J. Non-Cryst. Solids* **59&60**, 795 (1983).
- [12] C. C. Tsai, in: Hellmut Fritzsche (Ed.), *Amorphous Silicon and Related Materials*, World Scientific, Singapore, p.123, 1988.
- [13] I. Sieber, I. Urban, I. Dorfel, S. Koynov, R. Schwarz, M. Schmidt, *Thin Solid Films* **276**, 314 (1996).
- [14] Shaoyun Huang, Li Wang, Gautam Ganguly, Jun Xu, Xinfan Huang, Akihisa Matsuda, Kunji Chen, *Journal of Non-Crystalline Solids* **266-269**, 347 (2000).
- [15] Shaoyun Huang, Kunji Chen, Jianjun Shi, Xinfan Huang, Jun Xu, Gautam Ganguly, Akihisa Matsuda, *Jpn. J. Appl. Phys.* **40**, 40 (2001).
- [16] Li Wang, Jiang Yin, Shaoyun Huang, Xinfan Huang, Jun Xu, Zhiguo Liu, Kunji Chen, *Phys. Rev.* **B60**, R6976 (1999).